Indian Chemical Engineer

ISSN: 0019-4506 (Print) 0975-007X (Online) Journal homepage: https://www.tandfonline.com/loi/tice20

Palladium supported on nano-hybrid Zr–Al–La catalyst for hydrogenation of 2-ethylanthraquinone

Anjali A. Ingle, Shahid Z. Ansari, Diwakar Z. Shende, Kailas L. Wasewar & Aniruddha B. Pandit

To cite this article: Anjali A. Ingle, Shahid Z. Ansari, Diwakar Z. Shende, Kailas L. Wasewar & Aniruddha B. Pandit (2020): Palladium supported on nano-hybrid Zr–Al–La catalyst for hydrogenation of 2-ethylanthraquinone, Indian Chemical Engineer, DOI: 10.1080/00194506.2020.1749141

To link to this article: https://doi.org/10.1080/00194506.2020.1749141

Published online: 08 Apr 2020.

INDIAN CHEMICAL ENGINEER
https://doi.org/10.1080/00194506.2020.1749141

Palladium supported on nano-hybrid Zr–Al–La catalyst for hydrogenation of 2-ethylanthraquinone

Anjali A. Ingle[a], Shahid Z. Ansari[b], Diwakar Z. Shende[a], Kailas L. Wasewar[a] and Aniruddha B. Pandit[b]

[a]ASAL, Department of Chemical Engineering, VNIT, Nagpur, India; [b]Department of Chemical Engineering, ICT, Mumbai, India

ABSTRACT

Hydrogenation catalyst is of major importance in the production of eco-friendly oxidant hydrogen peroxide. Herein, in this work co-precipitation and an incipient wetness-impregnation method are used for the synthesis of Nano-hybrid (Zr–Al–La (ZAL)) supported Pd catalyst for the hydrogenation of 2-Ethylanthraquinone. The performance test of the developed catalyst was carried out in high-pressure autoclave reactor at 75°C and 0.3 MPa. It was found that the catalyst not only improved conversion of 2-ethylanthraquinone (93%) but also showed higher hydrogenation efficiency of 9.15 $g_{H_2O_2}/L$ with much lower concentration of the catalyst (0.5 g) at 75°C and 0.3 MPa compared to conventional catalysts Pd/PSC and Pd/PAC, which gave 4 g/L and 5 g/L respectively with 500 g of catalyst. Furthermore, the kinetic study indicated that the hydrogenation of 2-ethylanthraquinone found to be a zero and first order kinetics with respect to a 2-ethylanthraquinone concentration and H_2 concentration respectively. The activation energy was found to be 56.156 J/mol.

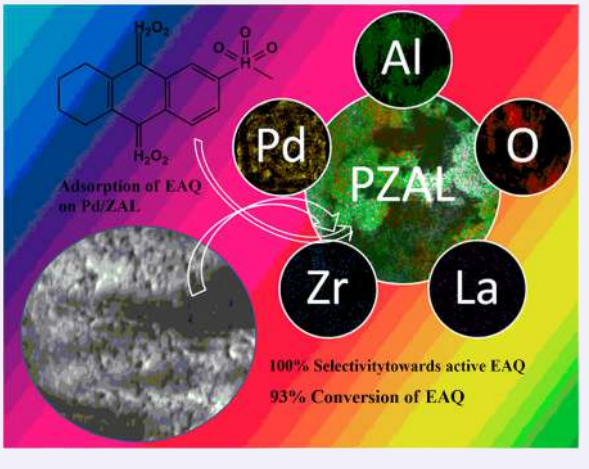

KEYWORDS

Palladium catalyst; 2-ethylanthraquinone hydrogenation; nano-hybrid support ZAL

CONTACT Aniruddha B. Pandit ab.pandit@ictmumbai.edu.in Department of Chemical Engineering, ICT, Mumbai 40019, India

Highlights

- Palladium supported on Zr-Al-La nanohybrid heterogeneous catalyst was developed and implemented in ecofriendly production of H_2O_2.
- Characterization and FESEM images confirmed its nanoporous morphology.
- The nanohybrid catalyst exhibited high conversion, hydrogenation efficiency, yield and selectivity in synthesis of hydrogen peroxide via anthraquinone route.

Notations

B	Hydrogenation efficacy (g/L)
C_{EAQ}	concentration of EAQ (mol/L)
C_{EAQ_0}	initial concentration of EAQ in working solution (mol/L)
C_{H_2}	concentration of H_2
C_{KMnO_4}	concentration of $KMnO_4$ solution (mol/L)
D	crystallite size of the particle (nm)
E	activation energy (J/mol)
k'	Constant Debye–Scherrer, $k' = 0.9$
k	rate constant (mol/h)
$M_{H_2O_2}$	molar mass of hydrogen peroxide (g/mol)
$n_{(H_2O_2)}$	moles of H_2O_2 formed (mol/L)
n_0(EAQ)	initial moles of 2-EAQ (mol/L)
$n_{(EAQ)}$	moles of 2-EAQ at time t (mol/L)
P_{H_2}	partial pressure of H_2 (MPa)
R	constant, $R = 8.314$ J/((mol K))
$-r_{EAQ}$	EAQ consumption rate (mol/h)
$-r_{H_2}$	H2 consumption rate (h^{-1})
r_{EAHQ}	EAHQ production rate (mol/h)
S	selectivity towards active quinones (%)
T	temperature (°C)
T	reaction time (h)
V_{KMnO_4}	volume of $KMnO_4$ solution (mL)
V	volume of hydrogen peroxide solution (mL)
x_{EAQ}	conversion of EAQ (%)
$Y_{H_2O_2}$	yield of H_2O_2 (%)
λ	wavelength of the incident X-ray radiation, $\lambda = 1.5406$ Å
β	full width at half maximum (FWHM) of the most intense peak
θ	Bragg's angle (radians)

1. Introduction

Hydrogen peroxides (H_2O_2) have a wide range of applications in the field of paper and pulp, oxidative chemical synthesis, mining, textile, waste water treatment, etc. due to its eco-friendly oxidising properties. More than 34% of its total production has been used in the pulp and paper industries as a bleaching agent and for washing of wool and cotton fibre in the textile industries. Hence, a significant research work on the synthesis of H_2O_2 is in progress. H_2O_2 is a natural metabolite of many organisms and hence, the only by-product formed from its decomposition is water and oxygen. [1–4]. The main raw material required for commercial production of H_2O_2 through auto-oxidation (AO) process is anthraquinone (AQ) derivatives, typically 2-ethylanthraquinone (2-EAQ) and tetrahydro-2-ethylanthraquinone. Scheme 1 depicted the systematic representation of the sequential hydrogenation and oxidation of an AQ derivative [5]. In a typical AO process, 2-ethylanthrahydroquinone (EAHQ) is formed through the hydrogenation of EAQ by dissolving it in a mixture of organic solvents. Further, oxidation of EAHQ leads to the formation of H_2O_2 and EAQ. Due to high solubility of H_2O_2 in water, it is extracted through the mixture using water as a solvent to recover H_2O_2 of various strength upto 50% concentration as an aqueous solution [6,7].

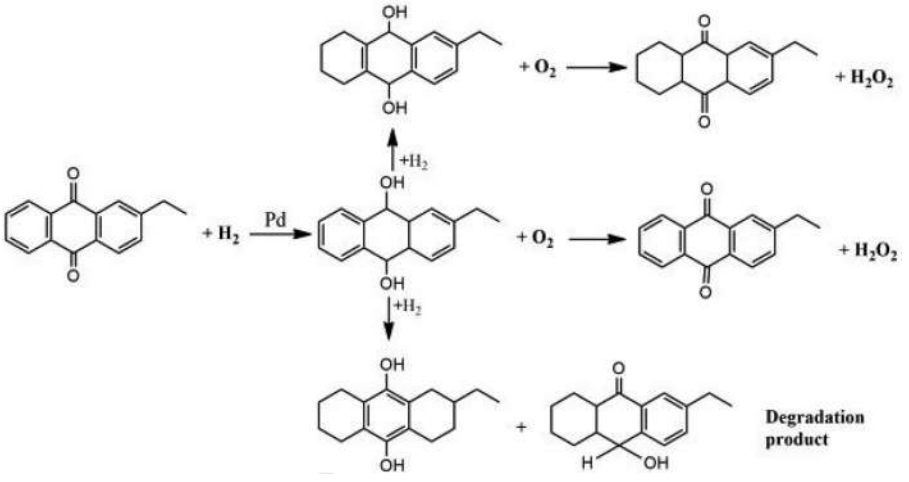

Scheme 1. A typical reaction of hydrogen peroxide through AQ process [5].

The catalytic hydrogenation of EAQ is of paramount importance in the synthesis of H_2O_2 through AQ route by using Pd catalyst, which has been seeking attention in the field of catalysis. Liu et al. [8] and Hou et al. [9] applied, Raney Nickel (Rn-Ni) catalyst for the catalytic hydrogenation of EAQ through AQ process. It was found that Pd catalyst has a great affinity towards hydrogenation reactions, hence Pd-supported catalysts are used in the industry instead of conventional Rn-Ni catalysts due to their higher activity and selectivity along with lower deactivation [8,9]. Pd on different supports, i.e. Al_2O_3, SiO_2 and SiO_2–Al_2O_3 has been used widely in the hydrogenation process. Hydrogenation reaction can be carried out as batch or as continuous operations. Therefore, the development of a highly active catalyst support with high selectivity to active quinines is one of the priority issues of the process improvement [7,10–17].

Besides, the hydrogenation of EAQ over Pd catalysts is a fast controlled by mass transfer process which was a fast reaction [18]. Hence, it is important to design a catalyst for hydrogenation reaction for EAQ which can lower the mass transfer resistance. Drelinkiewicz et al. and Kosydar et al. carried out sufficient work in the field of EAQ hydrogenation to investigate high-performance catalysts. It was found that silica-supported catalysts are more promising than alumina-supported catalyst in the hydrogenation reactions [19]. It was also found that the rate of reactions in the 'deep hydrogenation' stage decreases due to the addition of Na_2SiO_3, polyaniline or alkali modifiers (Li, Na, K, Cs) when used to modify the adsorption properties of the Al_2O_3 or SiO_2 support towards EAQ molecules [15]. There are different metal ions and metal alloys like Ni, Ni–Co, Pd, Pd–Au, Pd–Ru and Pd_3P supported on C, Al_2O_3, ZrO_2 and SiO_2 [5,6,8,9,15,20–22] for various hydrogenation reactions in the past. It is highly preferable to develop the existing catalyst structure to enhance the hydrogenation reaction of EAQ. The selectivity of supported Pd catalysts can be improved by adding promoters or by changing the nature of the supports. Pd is expensive and hence can be loaded on various supports such as PAN (SiO_2) composite, ZrO_2–γ–Al_2O_3, porous glass beads, Raschig ring alumina, Al_2O_3 and γ-Al_2O_3 prepared by oxidative polymerisation, deposition, impregnation, subcritical water treatment and ion exchange, wet impregnation, oil drop and impregnation and adsorption–reduction, respectively [16,23–27]. Supported Pd catalysts are easier for catalyst removal from the working solution than conventional catalysts making it more suitable to be used in the AQ process for the catalytic hydrogenation of the EAQ.

The current investigation in the field of mixed oxide supports has received considerable attention. The ZrO_2–Al_2O_3 oxides used as supports for catalysts have been reported [26]. Hou et al.

investigated the effects of lanthanum addition on Ni–B/γ-Al_2O_3 amorphous alloy catalysts used in EAQ hydrogenation [9]. It was found that the addition of different metals to existing supports can enhance the selectivity of the catalyst. Nano-hybrid catalysts (bimetallic and trimetallic) have been used for various hydrogenation reactions [27–33]. Herein, a novel nano-hybrid trimetallic catalyst support Zr–Al–La (ZAL) was synthesised by co-precipitation and impregnated with Pd by an incipient wetness-impregnation method. The co-precipitation by the direct contact of oxide supports gaining much attention due to its accessibility and economy. By this method of the preparation of trimetallic oxide support which precipitates with small size, narrow size distribution and high crystalline structure may be obtained. The excellent hydrogenation efficiency of Pd/ZAL catalyst can be rationalised as EAQ has an electrophilic properties and synthesised catalyst has nucleophilic reagent for the carbonyl groups in the EAQ structure. Hence, Pd/ZAL catalyst exhibits higher hydrogenation efficiency due to higher electron density because of the adsorption of electrophilic EAQ and nucleophilic Pd catalyst together. Catalytic activity of trimetallic nano-hybrid catalyst on the hydrogenation of EAQ was examined in a high-pressure autoclave reactor with the influence of different reaction parameters on the yield and hydrogenation efficiency of H_2O_2. Several analysis techniques including FTIR, FESEM-EDAX, BET and XRD were performed to investigate the catalytic performance of Pd/ZAL catalyst.

2. Experimental

2.1. Materials and methods

Palladium chloride ($PdCl_2$, Sigma Aldrich, purity >99.9%), zirconium oxychloride ($ZrOCl_2{\cdot}8H_2O$, LOBA Chemie, purity >99.9%), aluminium chloride ($AlCl_3$, Merck, purity >99.9%), lanthanum nitrate hexahydrate ($La(NO_3)_3{\cdot}6H_2O$, Merck, purity >99.9%), 2-ethyl-9,10-anthraquinone (EAQ, Alfa Aesar, purity >99.0%), anhydrous methanol (high-performance liquid chromatography (HPLC) grade, Merck, purity >99.9%), HPLC grade water (Merck), mesitylene (LOBA, purity >98.0%), trioctyl phosphate (TOP, Alfa Aesar, purity >96.0%), ethanol (Merck, purity >99.9%), xylene (Merck, purity >99.0%), potassium permanganate ($KMnO_4$, Merck, purity >98.0%), concentrated sulphuric acid (H_2SO_4, Merck, purity >98.0%) and concentrated nitric acid (HNO_3, Merck, purity >70.0%) were procured and used without further purification.

2.2. Preparation of nano-hybrid support (ZAL)

The ZAL nano-hybrid catalyst support was prepared by co-precipitation method. In this equimolar compositions of $AlCl_3$ (0.5 M), La $(NO_3)_3{\cdot}6H_2O$ (0.5 M) and $ZrOCl_2{\cdot}8H_2O$ (0.5 M) were dissolving in 100 mL Millipore water to prepare the mixed solution of ZAL support. The pH of this solution was adjusted to 9.5–10 by adding 5–6 drops per minute of ammonia solution (30% ammonia) to the mixed solution of ZAL. Attaining this pH, there is formation of precipitate in the solution. This precipitate was centrifuged and separated from the slurry. Further, it was neutralised by washing with Millipore water. It was later dried in a laboratory hot air oven for 72 h at 65°C. This powder was finely grounded in a mortar and pestle and stored in air tight container at room temperature.

2.3. Preparation of Pd/ZAL nano-hybrid catalysts

The $PdCl_2$ (500 mg/L) was loaded on ZAL nano-hybrid support at room temperature by an incipient wetness-impregnation technique. Ammonia solution was added drop wise with a continuous stirring until pH 12 was attained. Solution pH was maintained for 48 h at 150 rpm in an orbital shaker incubator at 27°C. The synthesised Pd/ZAL catalyst was washed with Millipore water and centrifuged to obtain a neutral pH of the filtrate and was tested by 1 wt.% $AgNO_3$ solution. Using hot air oven for

6 h at a temperature of 120°C, the Pd/ZAL catalyst was dried and calcined using muffle furnace for 2 h at 400°C. It was stored in an air tight container at room temperature.

2.4. Catalyst characterisation

Nano-hybrid catalyst was characterised using FTIR analysis, FESEM-EDAX, BET and XRD. FTIR analysis (Shimadzu Corporation IR-Affinity-1, Japan) was used to detect functional groups present on the surface of the catalyst. All spectra were recorded in the range of 400–4000 cm^{-1} at room temperature using KBr disc. Field-emission scanning electron microscopy with electronic X-ray diffraction (FESEM-EDAX) images of nano-catalyst was obtained using a field-emission scanning electron microscope (JSM 7600F). BET surface area was measured using NOVA touch 1F with nitrogen adsorption–desorption technique. Further, chemical composition of Pd–ZAL catalyst was ascertain by using PAN analytical X'PERT PRO X-ray diffractometer (XRD) in the 2θ range of 10°–100° with a step size of 0.01°, using a Cu X-Ray tube.

2.5. Catalyst activity test

The catalytic performance of Pd/ZAL catalyst in the hydrogenation of EAQ was performed using high-pressure autoclave reactor (50 mL) at 75°C and 0.3 MPa (Amar Equipment, Mumbai, Maharashtra, India). Working solution was prepared by combining EAQ (109 g/L) with mixing solvent, i.e. TOP and mesitylene with the volume ratio of 1:1. The Pd/ZAL nano-hybrid catalyst was reduced in the presence of H_2 flow in a high-pressure autoclave reactor at 0.3 MPa at 200°C for 2 h prior to the hydrogenation reaction. In each experiment, 30 mL of working solution was fed to the reactor while varying the catalyst dosages from 0.1 to 0.5 g (0.27–1.33 wt.%) at a constant pressure of 0.3 MPa. After hydrogenation, solution was instantaneously centrifuged at 4000 rpm for 5 min to isolate the solid catalyst. Thereafter, 2 mL of catalyst-free solution (EAHQ) was transferred into 20 mL of Millipore water to undergo oxidation with O_2 at atmospheric pressure and room temperature for 20 min. Concentration of H_2O_2 was analysed by adding 5 mL of 20 wt.% H_2SO_4 to 2 mL of aqueous oxidised solution followed by titration with a $KMnO_4$ solution [7–12,14,15].

Concentration of 2-EAQ in organic phase was examined by HPLC using a chromatograph (Agilent1200, USA) with DAD detector (254 nm), equipped with Zorbax C18 column. The mobile phases was the mixture of 80% methanol and 20% HPLC water. The retention time of standard EAQ was about 9.5 min and the peak was well recognised.

2.6. Determination of kinetic properties

$$\mathrm{EAQ} + \mathrm{H_2} \rightarrow \mathrm{EAHQ} \tag{1}$$

Reaction kinetics involve in the hydrogenation of EAQ according to the reaction given in Equation (1) as follows:

$$-r = -\frac{dC}{\mathrm{d}t} = k[C_{\mathrm{EAQ}}]^0\left[\frac{p_{\mathrm{H_2}}}{\mathrm{RT}}\right]^1 \tag{2}$$

Reactions were carried out at 75°C, 0.3 MPa hydrogen pressure throughout the experiments. In each experiment, 30 mL of EAQ solution and 0.1–0.5 g of catalyst was used. Overall consumption rate of EAQ and H_2 in the hydrogenation of EAQ was evaluated by measuring moles of EAQ and H_2 consumed per unit time (Equation (2)). The rate of liquid phase hydrogenation of EAQ over Pd–ZAL catalyst was investigated as a function of hydrogenation time (Equations

(3 and 4)).

$$-r_{\mathrm{EAQ}} = -\frac{\mathrm{d}C_{\mathrm{EAQ}}}{\mathrm{d}t} = k[C_{\mathrm{EAQ}}]^0 \tag{3}$$

$$-r_{\mathrm{H_2}} = -\frac{\mathrm{d}C_{\mathrm{H_2}}}{\mathrm{d}t} = -\frac{dP_{\mathrm{H_2}}}{(\mathrm{RT}).\mathrm{d}t} = \frac{k}{RT}[p_{\mathrm{H_2}}]^1 \tag{4}$$

Conversion of EAQ (x) is the ratio of the total number of EAQ moles reacted to the number of EAQ moles initially present in the reactor Equation (5):

$$x_{\mathrm{EAQ}}\ (\%) = \frac{n_0(\mathrm{EAQ}) - n_{(\mathrm{EAQ})}}{n_0(\mathrm{EAQ})} \times 100 \tag{5}$$

Yield of H_2O_2 (y) is the ratio of the number of moles of H_2O_2 at time t to the number of EAQ moles initially present in the reactor calculated as Equation (6):

$$y_{\mathrm{H_2O_2}}\ (\%)\ = n_{(\mathrm{H_2O_2})}/n_0(\mathrm{EAQ}) \times 100 \tag{6}$$

Hydrogenation efficiency of the catalyst (B) is grams of H_2O_2 produced by 1 L of working solution volume as given in Equation (7) [23,27]:

$$B = \frac{5C_{\mathrm{KMnO_4}} \times V_{\mathrm{KMnO_4}} \times M_{\mathrm{H_2O_2}}}{2V} \tag{7}$$

Selectivity of EAQ (S) is the ratio of total number of moles of EAQ and H_2 at time t to number of EAQ moles initially present in the reactor calculated by Equation (8) [34]:

$$S = \frac{n_{(\mathrm{EAQ})} + n_{(\mathrm{H_2O_2})}}{n_0(\mathrm{EAQ})} \times 100 \tag{8}$$

3. Results and discussions

3.1. Characterisation of Pd–ZAL

XRD analysis was done to know the crystalline structure of Pd loaded on ZAL catalyst and it is confirmed from Figure 1 that the supported catalyst is crystalline in nature. XRD pattern of ZAL supported catalyst indicating that the Pd/ZAL catalyst mainly composed of oxides of Alumina, Zirconia and Lanthanum. Also, there are some Pd peaks are available in the XRD patterns, it indicated that Pd is successfully loaded on the top of the ZAL support. Figure 1 shows primary phase monoclinic zirconia peaks were observed at $2\theta = 17.5°$, 28.36°, 49.3°, 53.7°, 60.9°, 64.4°, 68.1° and 78.5° (JCPDS: 00-007-0343). Peak at $2\theta = 29.6°$, 34.86°, 49.7°, 61°, 63°, 73.7° and 82.7° (JCPDS: 00-003-0640) corresponded to the cubical phase of zirconia. It confirmed that ZrO_2 were presenting in cubical as well as monoclinic phase [35]. Peaks at $2\theta = 19.33°$, 39.05°, 45.56° and 65.7° can be attributed to Al_2O_3 (JCPDS: 00-004-0875) [36] and the diffraction peaks at $2\theta = 19.1^o$, 27.9^o, 29.8^o, 44.9^o and 53.5^o were ascribed to La_2O_3 (JCPDS: 65-3185) [37]. Sharp peaks at angle $2\theta = 39°$, 45.5°, 68.2°, 82°, and 86.2° attributed to PdO phases, monoclinic and cubic (JCPDS: 87–0641 and 65-6174) [38,39]. Average particle size of Pd–ZAL catalyst estimated using Debye–Scherer equation (Equation (9)) was found to be 5.149 nm.

$$D = \frac{k\lambda}{\beta\cos\theta} \tag{9}$$

Specific surface area of the developed catalyst was found to be 114.64 m^2/g with BET. FESEM–EDX was used to analyse the surface morphology of the developed nano-hybrid catalyst. Figure 2 revealed that the surface of the catalyst had spherically agglomerated flakes but not furnished any information related to its porous structures. Elemental composition of synthesised nano-hybrid material was

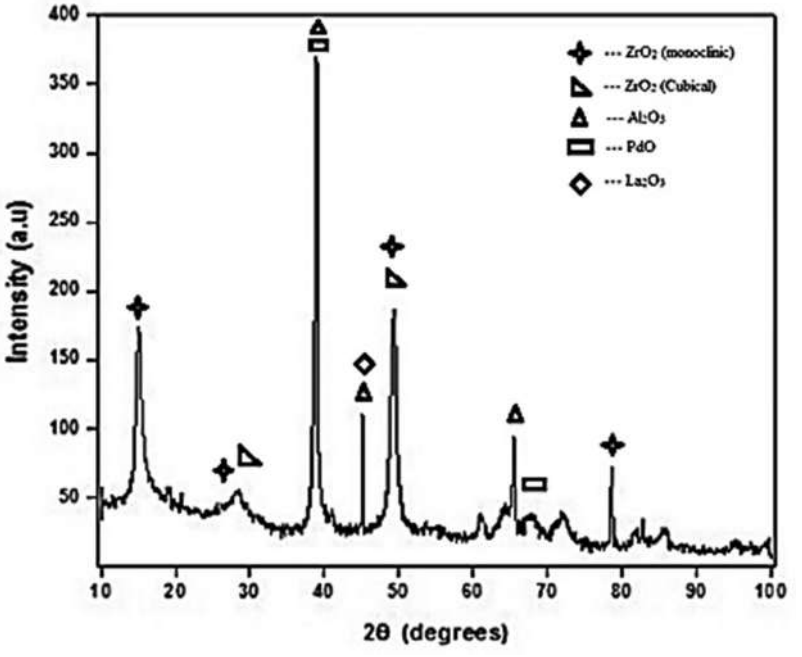

Figure 1. XRD patterns of Pd–ZAL catalyst.

identified by EDX spectroscopy attached with FESEM and well-defined peaks are seen in the EDX spectrum as can be seen in Figure 3. The EDAX spectrum indicates that the ZAL were mainly composed of Zirconia, Alumina and Lanthanum. From Figure 3, it was observed that Pd is also available in the EDAX spectrum, confirms that Pd was completely deposited on the ZAL support with size ranging under 100 nm.

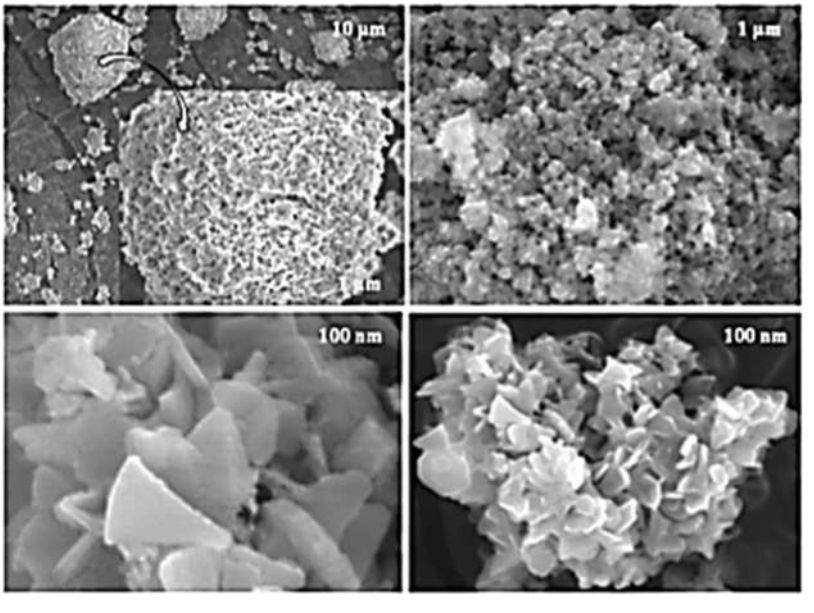

Figure 2. FESEM images of Pd–ZAL catalyst.

Figure 3. EDX spectrum of Pd–ZAL catalyst.

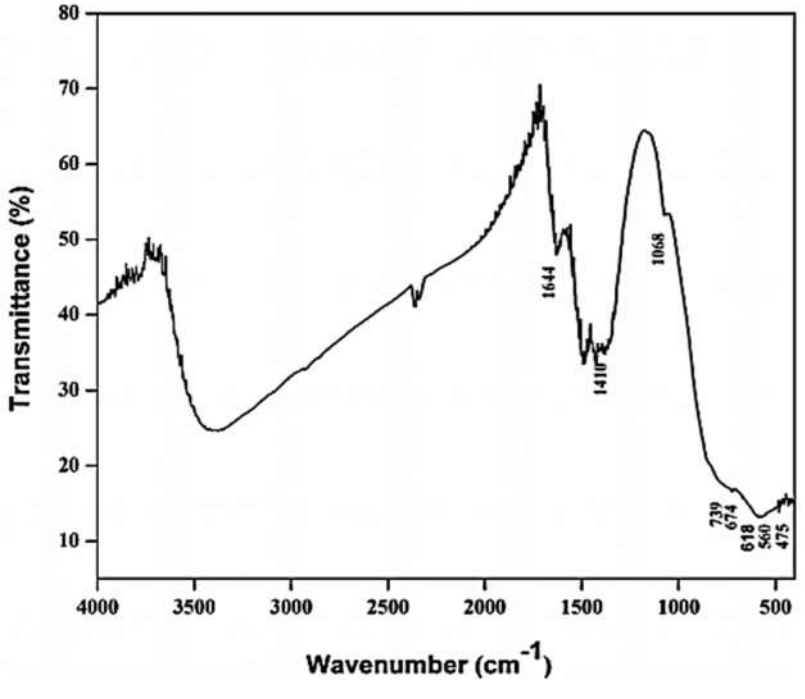

Figure 4. FTIR spectra of Pd–ZAL catalyst.

Fourier transforms infrared (FTIR) spectra of Pd–ZAL Nano-hybrid catalyst is illustrated in Figure 4. Vibration in the Al–O–Al bonds at 475 and 614 cm^{-1} position while peak position at 739 and 1068 cm^{-1} represents Al–O and O–H bonds, respectively. Peak at 674 and 560 cm^{-1}

could be due to La–OH bonds and the strong peak at 1410 cm^{-1} is due to Zr–OH bonds. Peak at 1644 cm^{-1} was due to the use of $PdCl_2$ in a reaction mixture [39].

3.2. Catalyst activity/performance test

3.2.1. Effect of reaction time

Catalytic hydrogenation experiments were performed to observe reaction kinetics of EAQ hydrogenation with respect to reaction time by varying the time from 0.5 to 2.66 h with initial EAQ concentration of 109 g/L at 75°C and 0.3 MPa in a high-pressure autoclave reactor by using a Pd–ZAL catalyst. Hydrogenation reaction of EAQ over supported Pd catalyst is zero order with respect to EAQ [18]. Plot of concentrations of EAQ per unit time was estimated to know the values of the rate constant using the integral method of analysis (Equation (3)). According to the integral method, Equation (3) can be rewritten as:

$$C_{EAQ_0} - C_{EAQ} = C_{EAQ_0} x_{EAQ} = kt \tag{10}$$

Rate constant k can be obtained from a plot of (x_{EAQ}) against reaction time (t) yield a straight line passing through origin with slope k is equal to 0.2 mol/Lh. Hence, it is confirmed that the hydrogenation reaction over as-prepared catalyst (Pd/ZAL) follows zero order for EAQ concentration and first order for H_2 concentration (Figure 5).

Conversion of EAQ increased rapidly with reaction time, particularly at the initial stage of hydrogenation and almost remained constant after 2.33 h. Maximum conversion of EAQ was 93% at 2.33 h over 0.5 g of catalyst. Conversion of EAQ as a function of reaction time over various catalyst supports is plotted in Figure 6. Hydrogenation experiments using highly active nano-hybrid catalyst (1.33 wt.% Pd/ZAL) provide higher performance among Al_2O_3- and SiO_2-supported Pd catalysts [17]. Conversion with 2 wt.% Pd/C and 1.33 wt.% Pd/ZAL were reported

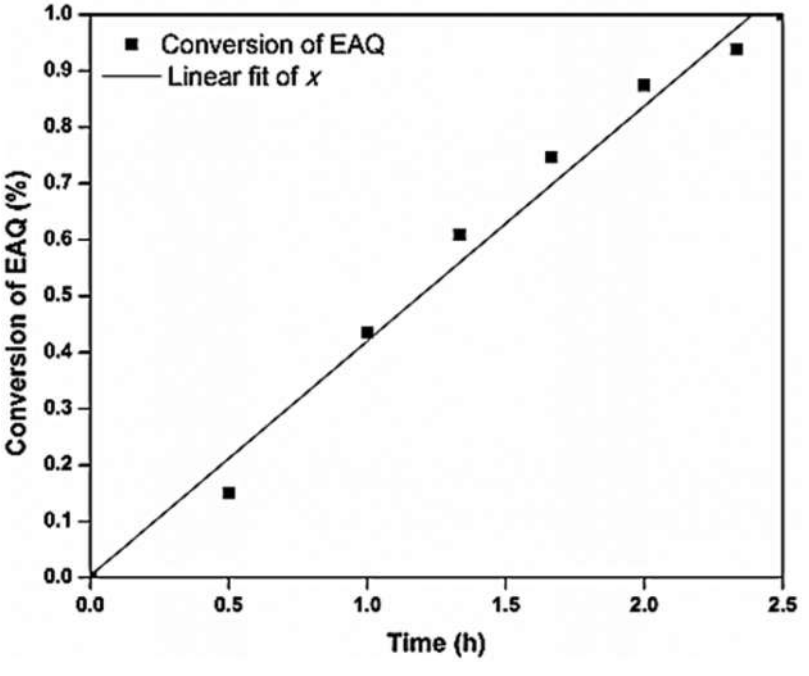

Figure 5. The hydrogenation of EAQ over kinetic catalyst at 75°C and 0.3 MPa (catalyst amount 0.5 g, initial EAQ concentration = 109 g/L and working solution volume = 30 mL).

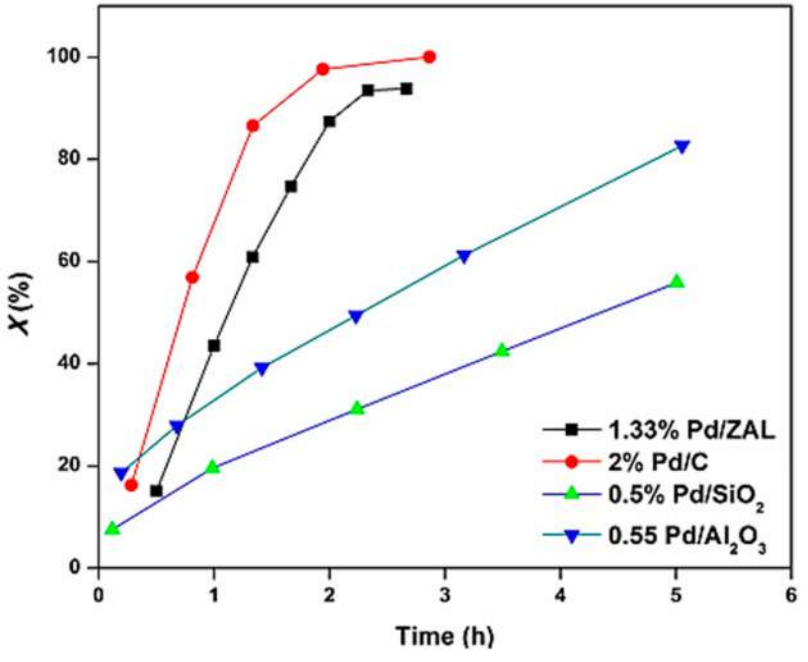

Figure 6. Conversion of 2-EAQ over different catalyst supports [17].

almost similar. Characteristics of Pd–ZAL catalyst in the hydrogenation of EAQ are compared in Table 1.

The effect of reaction time on hydrogenation efficiency and the yield of H_2O_2 are shown in Figure 7. Experiments were carried out with different reaction time, i.e. from 0.5 to 2.33 h with a constant volume of the working solution of 30 mL and catalyst dose of 0.5 g used in each batch. It was observed that the hydrogenation efficiency and the yield of H_2O_2 went on increasing initially and later on started tapering off with an increase in the reaction time. It was observed that for the reaction time of 2.33 h, a maximum yield of H_2O_2 achieved was 93.5% and a maximum hydrogenation efficiency observed was 9.15 $g_{H_2O_2}$/L. Increase in the reaction time did not have any significant effect on both the parameters. The excellent hydrogenation efficiency of Pd/ZAL catalyst can be rationalised as EAQ has electrophilic properties and synthesised catalyst has nucleophilic reagent for the carbonyl groups in the EAQ structure. Hence, Pd/ZAL catalyst exhibits higher hydrogenation efficiency due to higher electron density because of the adsorption of electrophilic EAQ and nucleophilic Pd catalyst together [24].

3.2.2. Effect of reaction temperature

Reaction kinetics of hydrogenated EAQ was investigated in terms of the effect of reaction temperature. Reaction temperature was varied from 50°C to 75°C. Relationship between yield and reaction

Table 1. Characteristics of catalysts in the hydrogenation of EAQ.

Items	Trickle-bed	Trickle-bed	High-pressure autoclave
Catalyst	Pd/PSC	GXH-1	Pd/ZAL
Catalyst amount	510 g	510 g	0.5 g
Solvents	TOP:C9–C10	TOP:C9–C10	TOP:TMB
Reaction parameters	0.3 MPa, 40°C	0.4 MPa, 40°C	0.3 MPa, 75°C
Hydrogenation efficiency	4–5$g_{H_2O_2}$/L [40]	5–6$g_{H_2O_2}$/L [25]	8–9 $g_{H_2O_2}$/L [ZAL]
Operation	Continuous; high cost	Continuous; high cost	Batch; moderate cost

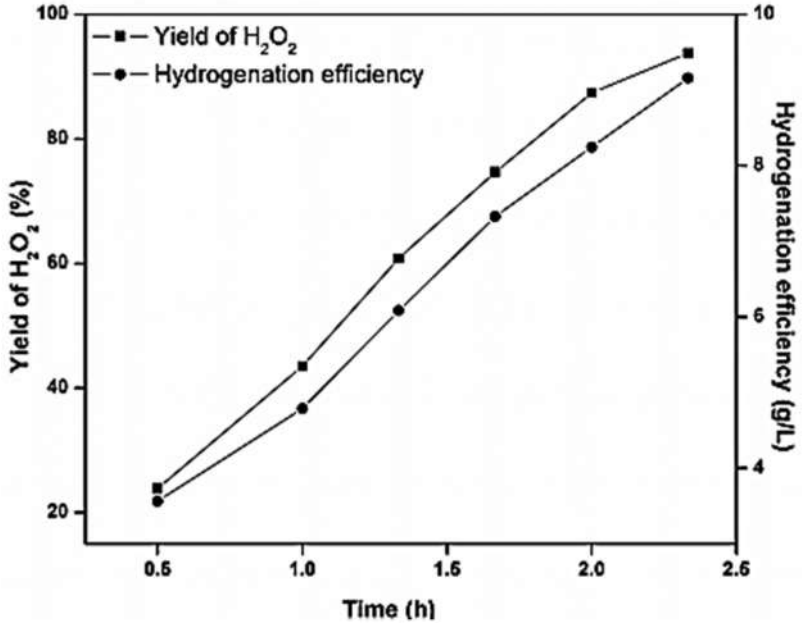

Figure 7. Yield of H_2O_2 and hydrogenation efficiency as a function of reaction time (working solution volume = 30 mL, temperature = 75°C, pressure = 0.3 MPa, initial concentration of EAQ = 109gL^{-1}, catalyst amount = 0.5 g).

time is given by Equation (11) [41].

$$\ln\left(\frac{1}{1-y}\right) = kt \tag{11}$$

Plot of $\ln(1/(1-y))$ versus reaction time (t) was drawn and is shown in Figure 8. Relationship between the yield and the reaction time was found to be linear. The R^2 values of each fitting line at temperatures of 50°C, 60°C, 70°C and 75°C were found to be 0.9657, 0.9703, 0.9495 and 0.9627 with slopes of 0.2946, 0.3705, 0.9394 and 1.3326.

Temperature dependency of rate constant can be evaluated by Arrhenius law as Equation (9). Rate constant (k) obtained from slope of Equation (11). Integrated form of Equation (9) to calculate the activation energy is given by Equation (10). Plot of $\ln(k)$ versus $1/T$ gives a linear line with R^2 value of 0.9941 it can be observed from Figure 9. Activation energy is found to be 56.156 J/mol.

$$k = k_0 e^{\left(-\frac{E}{RT}\right)} \tag{12}$$

$$\ln k = lnk_0 - \frac{E}{RT} \tag{13}$$

Figure 10 shows the effect of reaction temperature on the yield and hydrogenation efficiency of H_2O_2. Working solution volume and catalyst dosages were fixed at 30 mL and 0.5 g. It was observed that yield and hydrogenation efficiency were directly proportional to reaction temperature and went on increasing significantly with an increase in the temperature from 50°C to 75°C indicating that the reaction temperature plays an important role in the hydrogenation of EAQ due to temperature dependency of rate constant. As we increase the temperature, reaction rate constant and H_2 solubility both are also increased.

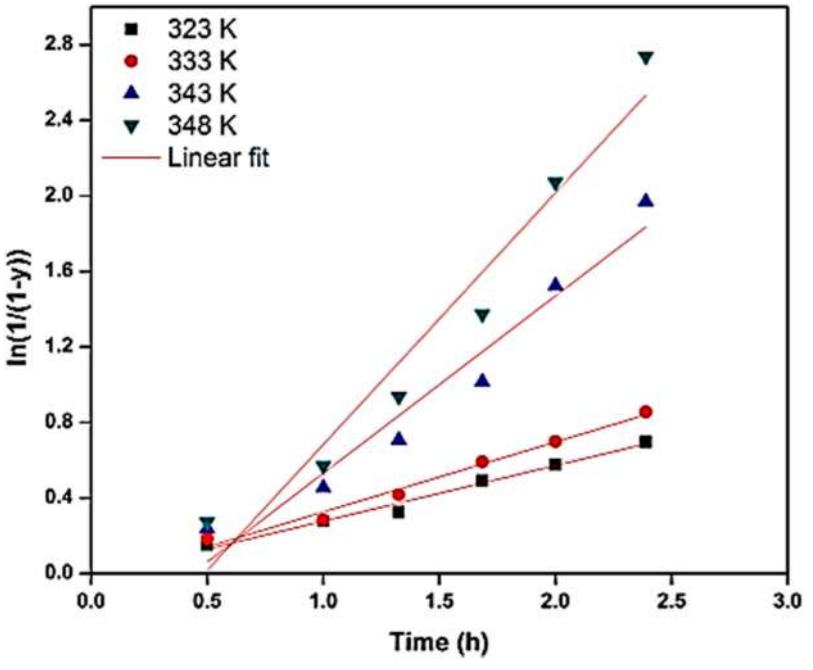

Figure 8. Plot of $\ln(1/(1-y))$ vs. reaction time.

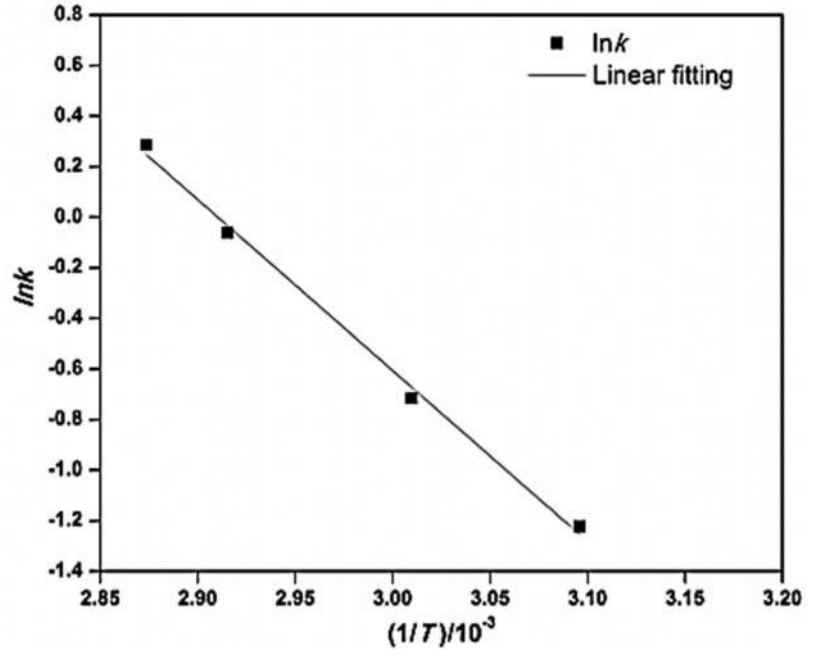

Figure 9. Plot of *lnk* versus 1/*T*.

3.2.3. Effect of solution volume

Figure 11 presents the effect of working solution volume against the yield of H_2O_2 and hydrogenation efficiency at constant catalyst dosages (0.5 g) and EAQ concentration (109 g/L). It is observed from the

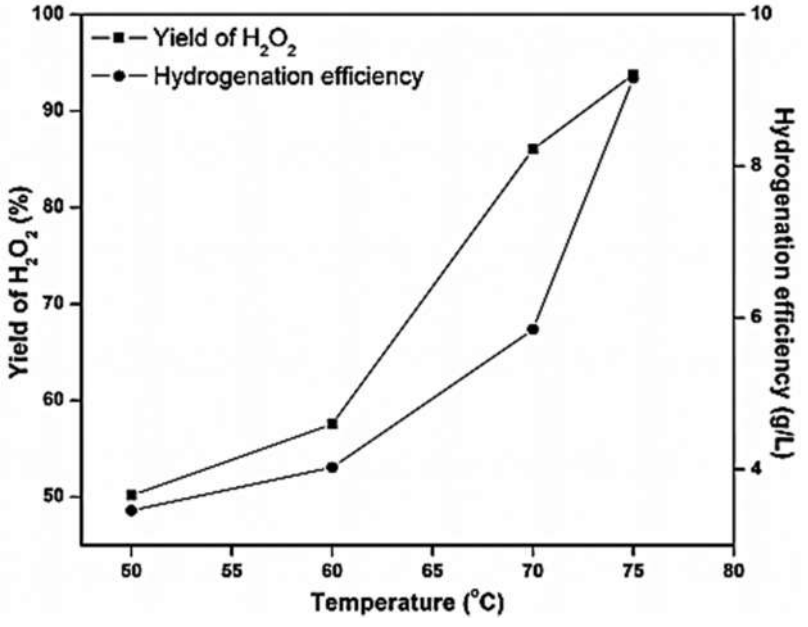

Figure 10. Yield of H_2O_2 and hydrogenation efficiency as a function of reaction temperature (working solution volume = 30 mL, temperature = 75°C, pressure = 0.3 MPa, initial concentration of EAQ = 109g.L^{-1}, catalyst amount = 0.5 g).

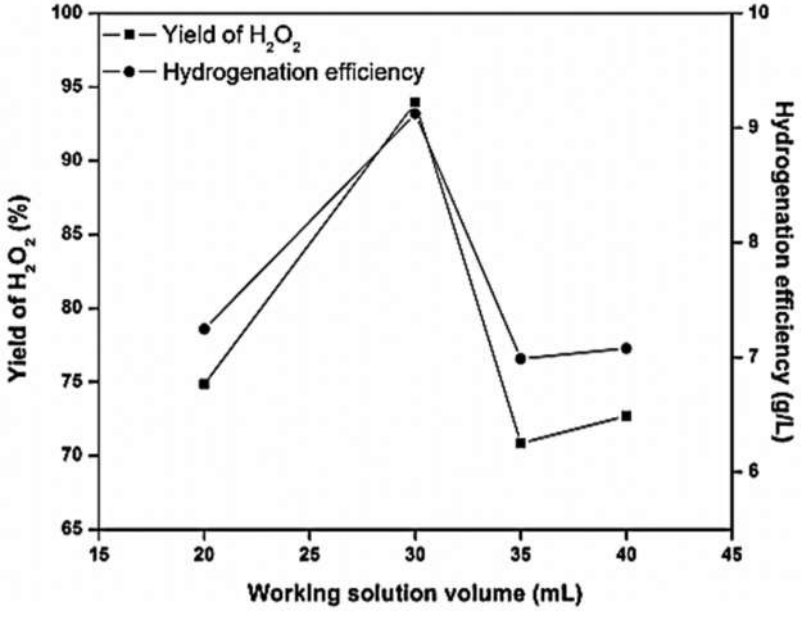

Figure 11. Yield of H_2O_2 and hydrogenation efficiency as a function of working solution volume (temperature = 75°C, pressure = 0.3 MPa, initial concentration of EAQ = 109 g.L^{-1}, catalyst amount = 0.5 g).

plot that the highest hydrogenation efficiency and the yield of H_2O_2 are obtained at the working solution volume of 30 mL. Working solution volume is directly proportional to the catalyst concentration and gas–liquid interface. If we increase the working solution volume, the catalyst concentration will be less and more gas–liquid interfaces will be available. On the other hand, when working solution volume was less than 30 mL, the formation of degradation product resulted because of less EAQ volume and an

active intermediate due to low gas–liquid interface. Hence, the yield and hydrogenation efficiency at 20 mL were less than the 30 mL working solution volume. In contrast, when working solution volume was more than 30 mL both the yield and hydrogenation efficiency were degraded to lower values. Hence, the working solution volume that plays an optimum role in the hydrogenation of EAQ was confirmed and it was fixed to the optimum value of 30 mL at a constant pressure of H_2 0.3 MPa.

4. Conclusions

The study on the performance of hydrogenation of 2-EAQ to EAHQ for the production of H_2O_2 was carried out by employing the synthesised Pd–ZAL Nano-hybrid catalyst. 2-EAQ liquid phase hydrogenation efficacy and yield of H_2O_2 over Nano-hybrid catalyst was studied against reaction time, temperature, working volume and catalyst dosages. Pd–ZAL catalyst improves the catalytic activity (9.15 g/L) and provides the high selectivity (100%) simultaneously, which has ascendancy over existing processes. The hydrogenation of 2-EAQ provides the conversion as high as 93% with only 0.5 g of the catalyst with a hydrogenation efficiency of 9.15 $g_{H_2O_2}$/L at operating conditions of 75°C and 0.3 MPa, respectively. The H_2O_2 achieved the highest yield of 93.5% at 2.33 h for 0.5 g of catalyst. The reaction was found to be the zero order with a concentration of EAQ and first order with respect to H_2 as we found the linear relationship between the yield H_2O_2 and the reaction time. The Pd–ZAL catalyst has shown scintillating performance and amicable for the hydrogenation of 2-EAQ.

5. Patents

A Hydrogenation catalyst and Process Thereof, India 201821004343-A, 2018/02/16.

Disclosure statement

No potential conflict of interest was reported by the author(s).

References

[1] Campos-Martin J.M., Blanco-Brieva G. and Fierro J.L.G., *Angew Chemie Int. Ed.*, **45**, pp. 6962 (2006).
[2] Han Y., He Z., Wang S., Li W. and Zhang J., *Catal. Sci. Technol.*, **5**, pp. 2630 (2015).
[3] Melada S., Rioda R., Menegazzo F., Pinna F. and Strukul G., "Direct Synthesis of Hydrogen Peroxide on Zirconia-Supported Catalysts Under Mild Conditions", *J. Catal.*, **239**, pp. 422–430 (2006).
[4] García-Serna J., Moreno T., Biasi P., Cocero M.J., Mikkola J.P. and Salmi T.O., "Engineering in Direct Synthesis of Hydrogen Peroxide: Targets, Reactors and Guidelines for Operational Conditions", *Green Chem.*, **16**, pp. 2320 (2014).
[5] Ya H., Shen C., Wang Y. and Luo G., "Catalytic Hydrogenation of 2-Ethylanthraquinone Using an In Situ Synthesized Pd Catalyst", *RSC Adv.*, **6**, pp. 23942–23948 (2016).
[6] Fang J., Chen X., Liu B., Yan S., Qiao M., Li H., He H. and Fan K., "Liquid-Phase Chemoselective Hydrogenation of 2-Ethylanthraquinone Over Chromium-Modified Nanosized Amorphous Ni–B Catalysts", *J. Catal.*, **229**, pp. 97–104 (2005).
[7] Chen Y., Wang L., Lu S., Wang Y. and Mi Z., *Ind. Eng. Chem. Res.*, **47**, pp. 7414 (2008).
[8] Liu B., Qiao M., Deng J.F., Fan K., Zhang X. and Zong B., "Skeletal Ni Catalyst Prepared From a Rapidly Quenched Ni–Al Alloy and Its High Selectivity in 2-Ethylanthraquinone Hydrogenation", *J. Catal.*, **204**, pp. 512–515 (2001).
[9] Hou Y., Wang Y., He F., Mi W., Li Z., Mi Z., Wu W. and Min E., "Effects of Lanthanum Addition on Ni-B/γ-Al2O3 Amorphous Alloy Catalysts Used in Anthraquinone Hydrogenation", *Appl. Catal., A*, **259**, pp. 35–40 (2004).
[10] Isaka Y., Yamada Y., Suenobu T., Nakagawa T. and Fukuzumi S., "Production of Hydrogen Peroxide by Combination of Semiconductor-Photocatalysed Oxidation of Water and Photocatalytic Two-Electron Reduction of Dioxygen", *RSC Adv.*, **6**, pp. 42041–42044 (2016).
[11] Freakley S.J., He Q., Harrhy J.H., Lu L., Crole D.A., Morgan D.J., Ntainjua E.N., Edwards J.K., Carley A.F. and Borisevich A.Y., "Palladium-tin Catalysts for the Direct Synthesis of H2O2 with High Selectivity", *Science*, **351** (80), pp. 965–968 (2016).

[12] Hong R., Feng J., He Y. and Li D., "Controllable Preparation and Catalytic Performance of Pd/Anodic Alumina Oxide@Al Catalyst for Hydrogenation of Ethylanthraquinone", *Chem. Eng. Sci.*, **135**, pp. 274–284 (2015). doi:10.1016/j.ces.2015.04.003.
[13] Li Y., Feng J., He Y., Evans D.G. and Li D., *Ind. Eng. Chem. Res.*, **51**, pp. 11083 (2012).
[14] Liu G., Duan Y., Wang Y., Wang L. and Mi Z., *Chem. Eng. Sci.*, **60**, pp. 6270 (2005).
[15] Kosydar R., Drelinkiewicz A., Lalik E. and Gurgul J., "The Role of Alkali Modifiers (Li, Na, K, Cs) in Activity of 2%Pd/Al2O3 Catalysts for 2-Ethyl-9,10-Anthraquione Hydrogenation", *Appl. Catal., A*, **402**, pp. 121–131 (2011).
[16] Drelinkiewicz A., Waksmundzka-Góra A., Makowski W. and Stejskal J., *Catal. Commun.*, **6**, pp. 347 (2005).
[17] Drelinkiewicz A. and Waksmundzka-Góra A., "Investigation of 2-Ethylanthraquinone Degradation on Palladium Catalysts", *J. Mol. Catal. A: Chem.*, **246**, pp. 167–175 (2006).
[18] Santacesaria E., Di Serio M., Russo A., Leone U. and Velotti R., *Chem. Eng. Sci.*, **54**, pp. 2799 (1999).
[19] Drelinkiewicz A., Pukkinen A., Kangas R. and Laitinen R., *Catal. Lett.*, **94**, pp. 157 (2004).
[20] Chen X., Hu H., Liu B., Qiao M., Fan K. and He H., "Selective Hydrogenation of 2-Ethylanthraquinone Over an Environmentally Benign Ni_B/SBA-15 Catalyst Prepared by a Novel Reductant–Impregnation Method", *J. Catal.*, **220**, pp. 254–257 (2003).
[21] Lu C., Zhu Q., Zhang X., Liu Q., Nie J., Feng F., Zhang Q., Ma L., Han W. and Li X., "Preparation and Catalytic Performance of Metal-Rich Pd Phosphides for the Solvent-Free Selective Hydrogenation of Chloronitrobenzene", *Catalysts*, **9**, pp. 177 (2019).
[22] Shi Y., Chen S., He L., Ning P. and Guan Q., "Selective Conversion of Phenol in a Subcritical Water Medium Using γ-Al2O3 Supported Ni–Co Bimetallic Catalyst", *Catalysts*, **9**, pp. 212 (201)..
[23] Wang F., Xu X. and Sun K., *React. Kinet. Catal. Lett.*, **93**, pp. 135 (2008).
[24] Shen C., Wang Y.J., Xu J.H., Lu Y.C. and Luo G.S., *Chem. Eng. J.*, **173**, pp. 226 (2011).
[25] Shang H., Zhou H., Zhu Z. and Zhang W., *J. Ind. Eng. Chem.*, **18**, pp. 1851 (2012).
[26] Tang P., Chai Y., Feng J., Feng Y., Li Y. and Li D., "Highly Dispersed Pd Catalyst for Anthraquinone Hydrogenation Supported on Alumina Derived From a Pseudoboehmite Precursor", *Appl. Catal., A*, **469**, pp. 312–319 (2014).
[27] Chen H., Huang D., Su X., Huang J., Jing X., Du M., Sun D., Jia L. and Li Q., *Chem. Eng. J.*, **262**, pp. 356 (2015).
[28] Carvalho L.S., Pieck C.L., Rangel M.C., Fígoli N.S., Vera C.R. and Parera J.M., "Trimetallic Naphtha Reforming Catalysts", *Appl. Catal., A*, **269**, pp. 105–116 (2004).
[29] Surisetty V.R., Dalai A.K. and Kozinski J., "Intrinsic Reaction Kinetics of Higher Alcohol Synthesis From Synthesis Gas Over a Sulfided Alkali-Promoted Co−Rh−Mo Trimetallic Catalyst Supported on Multiwalled Carbon Nanotubes (MWCNTs)", *Energy Fuels*, **24**, pp. 4130–4137 (2010).
[30] Hungria A.B., Raja R., Adams R.D., Captain B., Thomas J.M., Midgley P.A., Golovko V. and Johnson B.F.G., *Angew Chemie Int Ed*, **45**, pp. 4782 (2006).
[31] Toshima N., Ito R., Matsushita T. and Shiraishi Y., "Trimetallic Nanoparticles Having a Au-Core Structure", *Catal. Today*, **122**, pp. 239–244 (2007).
[32] Adams R.D., Boswell E.M., Captain B., Hungria A.B., Midgley P.A., Raja R. and Thomas J.M., *Angew Chemie Int Ed*, **46**, pp. 8182 (2007).
[33] Liew K.H., Lee T.K., Yarmo M.A., Loh K.S., Peixoto A.F., Freire C. and Yusop R.M., "Ruthenium Supported on Ionically Cross-Linked Chitosan-Carrageenan Hybrid MnFe2O4 Catalysts for 4-Nitrophenol Reduction", *Catalysts*, **9**, pp. 254 (2019).
[34] Li X., Su H., Ren G. and Wang S., "The Role of MgO in the Performance of Pd/SiO2/Cordierite Monolith Catalyst for the Hydrogenation of 2-Ethyl-Anthraquinone", *Appl. Catal., A*, **517**, pp. 168–175 (2016).
[35] Naeem M.A., Al-Fatesh A.S., Fakeeha A.H. and Abasaeed A.E., "Hydrogen Production From Methane dry Reforming Over Nickel-Based Nanocatalysts Using Surfactant-Assisted or Polyol Method", *Int. J. Hydrogen Energy*, **39**, pp. 17009–17023 (2014).
[36] Fakeeha A.H., Naeem M.A., Khan W.U. and Alfatesh A.S., *J. Ind. Eng. Chem.*, **20**, pp. 549 (2014).
[37] Wang J., Kang D., Yu X., Ge M. and Chen Y., "Improved Fruit fly Optimization Algorithm Optimized Wavelet Neural Network for Statistical Data Modeling for Industrial Polypropylene Melt Index Prediction", *J. Chemom.*, **29**, pp. 506–513 (2015).
[38] Karthikeyan B. and Loganathan B., "Rapid Green Synthetic Protocol for Novel Trimetallic Nanoparticles", *Journal of Nanoparticles*, **2013**, pp. 1–8 (2013).
[39] Vilas V., Philip D. and Mathew J., *Mat Chem Phys*, **170**, pp. 1 (2016).
[40] Li X., Su H., Ren G. and Wang S., "A Highly Stable Pd/SiO_2/Cordierite Monolith Catalyst for 2-Ethyl-Anthraquinone Hydrogenation", *RSC Adv.*, **5**, pp. 100968 (2015).
[41] Yao H., Shen C., Wang Y. and Luo G., "Catalytic Hydrogenation of 2-Ethylanthraquinone using an in situ Synthesized Pd Catalyst", *RSC Adv.*, 6, pp. 23942–23948 (2016).